Influence of electromagnetic fields on the generation of the directed and elliptic flows of heavy quarks in relativistic heavy-ion collisions

Santosh K. Das,[1,2] Olga Soloveva,[3] Taesoo Song,[3] and Elena Bratkovskaya[2,3,4]
[1]*School of Physical Sciences, Indian Institute of Technology Goa, Ponda-403401, Goa, India*
[2]*Helmholtz Research Academy Hesse for FAIR (HFHF), GSI Helmholtz Center for Heavy Ion Research, Campus Frankfurt, 60438 Frankfurt, Germany*
[3]*GSI Helmholtzzentrum für Schwerionenforschung GmbH, Planckstrasse 1, D-64291 Darmstadt, Germany*
[4]*Institut für Theoretische Physik, Johann Wolfgang Goethe-Universität, Max-von-Laue-Str. 1, D-60438 Frankfurt am Main, Germany*

(Received 1 August 2025; accepted 20 October 2025; published 1 December 2025)

We study the impact of self-generated electromagnetic fields (EMF) on the momentum evolution of charm quarks in the partonic and hadronic medium created in heavy-ion collisions at energies available at the Relativistic Heavy Ion Collier (RHIC), using the parton-hadron-string dynamics (PHSD) off-shell transport approach. In the quark-gluon plasma (QGP) phase, the charm quark interacts with the off-shell partons, whose mass and widths are given by the dynamical quasiparticle model (DQPM), which can reproduce the lattice QCD thermodynamics. The background electromagnetic fields are computed dynamically within the PHSD considering both the spectators and participants protons as well as newly produced charged hadrons, quarks, and antiquarks, which reflects naturally the electric conductivity $\sigma_{\rm el}$ of the medium. We study the directed and elliptic flow of D mesons in the presence of electromagnetic fields. We find that electromagnetically induced v_1 splitting in the D meson through D^0 and $\overline{D}^0$ mesons is consistent with the experimental data. Furthermore, we notice that the v_1 splitting in the heavy quark as a function of p_T is more prominent as a probe of the produced electromagnetic fields. However, we find only a small impact of electromagnetic fields on the heavy quark elliptic flow v_2.

DOI: 10.1103/yppc-ts4n

I. INTRODUCTION

According to the fundamental theory of strong interactions, quantum chromodynamics (QCD), at high temperature and density, nuclear matter changes its phase: hadrons dissolve to interacting quarks and gluons, the quark-gluon plasma (QGP) [1,2]. Relativistic heavy-ion collisions at the Relativistic Heavy Ion Collider (RHIC) and the Large Hadron Collider (LHC) are the experiments used to realize such extreme conditions of temperature and density.

To characterize the QGP, penetrating and well-calibrated probes are extremely important, and in this context heavy quarks (HQs), mainly charm (c) and bottom (b) quarks, play a crucial role [3–10]. Due to their larger mass (M), compared to the temperature (T), they are expected to be created early at energies available at the RHIC and LHC. HQ thermal production in the QGP can be neglected because of Boltzmann suppression ($\approx e^{-M/T}$); this ensures nearly exact flavor conservation during the evolution of the QGP. Since the thermalization time of heavy quarks is delayed relative to the light partons of the bulk medium by a factor of order $\approx M/T$, heavy flavor particles are not expected to be fully thermalized, and therefore they preserve a memory of their interaction history in both the initial stage and the subsequent evolution into the QGP phase. One of the prime goals of hard probe research is to quantify the spatial diffusion constant, D_s, of heavy quarks, a measure of the interaction strength of heavy quarks with the bulk medium. The collective properties of the D meson have been measured at both RHIC and LHC energies through the nuclear suppression factor R_{AA} and elliptic flow v_2. Several attempts [11–30] have been made to study both observables simultaneously, which can constrain the heavy quark diffusion coefficient.

In the recent past, it was recognized that extremely intense electromagnetic fields [31,32] are produced in noncentral heavy-ion collisions mainly due to the motion of spectator charges. The strength of the initial magnetic field produced at the very early stage of collisions at RHIC and LHC energies can be up to $eB \approx (5\text{–}50)m_\pi^2$, which is about a few orders of magnitude larger than that expected to be produced at the surface of magnetars. Once the two spectator charges recede from each other, the magnetic fields decay, which in return generates an electric field. Heavy-ion collisions at RHIC and LHC energies provide a unique opportunity to study physics under extremely high electromagnetic fields. Heavy quarks are considered to be a novel probe of this electromagnetic field because they are produced early, and, being a nonequilibrium probe, they will be able to retain the interaction history till its detection as heavy mesons in experiments. The directed flow v_1 of heavy mesons [33–41] is considered to be a

Published by the American Physical Society under the terms of the Creative Commons Attribution 4.0 International license. Further distribution of this work must maintain attribution to the author(s) and the published article's title, journal citation, and DOI.

promising observable to characterize the generated electromagnetic fields. Heavy quark directed flow is predicted [33] to be an order of magnitude larger than light hadron directed flow. However, to disentangle other sources of the directed flow, electromagnetically induced splitting in the directed flow, between positively and negatively charged quarks, of charm and anticharm quarks through D^0 and $\overline{D}^0$ mesons (also D^- and D^+) is considered to be a novel observable to scrutinize and quantify the initial electromagnetic field.

Recently both STAR [42] and ALICE [43] Collaborations measured the directed flow of D mesons at RHIC and LHC energies. Both collaborations obtained a finite directed flow that is an order of magnitude larger than that of the light hadrons. The measured splitting in the directed flow through D^0 and $\overline{D}^0$ mesons $[\Delta v_1 = v_1(D^0) - v_1(\overline{D^0})]$ at the highest RHIC center-of-mass energy $\sqrt{s_{NN}} = 200$ GeV fluctuates around zero and is smaller than the current precision of the experimental measurements. On the other hand, the slope of the directed flow splitting measured at LHC energy is positive, and its magnitude is about three orders of magnitude larger than that of the light charged hadrons.

So far, from the theoretical side, only very few attempts have been made to study the D meson directed flow. Many models obtained a finite but negative slope for the D meson directed flow splitting at both RHIC and LHC energies [33–35]. Recently, it was shown that a positive slope of D meson directed flow splitting at LHC energy can be obtained only if the magnetic field dominates over the electric field [38,40]. However, it was done in an *ad hoc* way to investigate a potential scenario yielding a positive slope. The time evolution of the electromagnetic field plays an important role in setting the sign of the slope of a directed flow splitting. The models currently employed to evaluate the electromagnetic field to compute heavy quark directed flow involve several approximations. Moreover, the electrical conductivity—an essential parameter for modeling the time evolution of the electromagnetic field in QCD matter—remains subject to significant uncertainties.

The heavy-quark diffusion coefficients in the presence of a magnetic field have been computed by several groups [44–51] in both the static and dynamic limits. These studies employ different approximations, such as the strong-field case within the lowest Landau level approximation [44–47], the weak-field case using a perturbative expansion in powers of eB [48,51], and the more general case for an arbitrary magnetic field strength [49]. The presence of a magnetic field induces anisotropy, leading to a decomposition of the heavy-quark diffusion coefficients [44,45]. In the weak-field limit, the heavy-quark diffusion coefficient increases with the magnetic field strength compared to the case without a magnetic field, although the effect is small. However, in the strong-field limit, and for an arbitrary magnetic field, the effect can become sizable. Further details can be found in Refs. [47–49,51].

The goal of this study is to investigate the influence of electromagnetic fields on charm directed and elliptic flow based on a consistent dynamical description of charm degrees of freedom (on quark and hadron levels) and their interactions in the partonic and hadronic medium, where electromagnetic fields are self-generated in a dynamical way during the time evolution of heavy-ion collisions. Our study is based on parton-hadron-string dynamics (PHSD) [52–57], which is a microscopic covariant dynamical approach for strongly interacting systems formulated on the basis of off-shell Kadanoff-Baym equations, and describes the space-time evolution of the matter, starting from the initial hard collisions until kinetic freeze-out, produced in high energy heavy-ion collisions. The description of the QGP is done within the dynamical quasiparticle model (DQPM) [53,56–60] which is an effective field-theoretical model for the description of nonperturbative QCD phenomena and reproduces the lattice QCD thermodynamical results based on covariant propagators for quarks/antiquarks and gluons that have a finite width in their spectral functions (imaginary parts of the propagators). The background electromagnetic fields created in high energy heavy-ion collisions due to both the spectators and participants are taken into account dynamically within the PHSD by including an electromagnetic tensor into the transport equations [32,36,61–65]. Moreover, PHSD can also describe the heavy quark observables at both RHIC and LHC energies [23,25]. In the present work, we study the impact of the electromagnetic field on heavy quark observables, mainly heavy quark directed and elliptic flows within the framework of PHSD in the presence of the electromagnetic field.

The paper is organized as follows. In Sec. II we represent the PHSD transport setup used in this calculation. In Sec. III we resent the electromagnetic field evolution within PHSD. In Sec. IV we present the results on heavy quark directed and elliptic flows. Finally, Sec. V is devoted to a summary of our study.

II. THE HEAVY FLAVORS PRODUCTION IN THE PHSD TRANSPORT APPROACH

In parton-hadron-string dynamics (PHSD) [52–57], the heavy flavor is produced through initial nucleon-nucleon hard scattering. Its energy-momentum is given by the pythia event generator and its spatial position by the Glauber model [23,25]. The rapidity distribution and transverse momentum from pythia are then rescaled such that they are consistent with those from the fonll calculations [23,66]. The parton distribution in heavy-ion collisions is modified compared to a static nucleon. As a result, heavy quark distribution, which is a byproduct of the hard scattering of partons, also changes. These (anti)shadowing effects are realized through the EPS09 parametrization [67] in PHSD [25]. After production, heavy quarks interact with thermal partons, which are massive off-shell particles within the dynamical quasiparticle model (DQPM) [68]. The pole mass and spectral width of the thermal partons depend on the properties of QGP, such as temperature and baryon chemical potential [57]. They take the form of hard thermal loop calculations, and the strong coupling is parametrized such that the lattice equation of state (EoS) is reproduced at both zero and nonvanishing baryon chemical potentials. The scattering cross section of heavy quarks with thermal partons is calculated by leading-order Feynman diagrams. However, propagators in the diagram have nonzero

pole mass and width, which makes the results divergence free, and resummation of Feynman diagrams is effectively included [68].

Once the local energy density is below 0.75 GeV/fm^3, heavy quarks coalesce toward hadronization [23]. First, all possible combinations of a heavy quark and light antiquark are taken into account by calculating the coalescence probability, which depends on momentum and spatial distances between the partons in the center-of-mass frame. In the Monte Carlo method, it is then decided whether coalescence takes place or not. If the coalescence happens, a coalescence partner is selected among all candidates by Monte Carlo based on the coalescence probability of each pair. This process is repeated until the energy density is lower than 0.4 GeV/fm^3. If a heavy quark still fails to coalesce, it is forced to hadronize by the fragmentation as in *pp* collisions [69]. The coalescence probability is large at low transverse momentum but small at large transverse momentum because of a poor overlap of the heavy quark and the light antiquark in momentum space. For the heavy quark fragmentation, PHSD adopts the Peterson fragmentation function. After hadronization, a heavy meson interacts with light meson or light baryon. The scattering cross sections are calculated on the basis of a chiral effective Lagrangian with unitarization energies [70].

It is found that the production and dynamics of heavy flavors ($D/\bar{D}$ and $B/\bar{B}$ mesons) in PHSD is consistent with experimental observables (such as rapidity and p_T spectra, R_{AA} ratios, elliptic flow v_2 coefficients) from the RHIC beam energy scan (BES) and from the Large Hadron Collider (LHC) [23,25,71–74].

III. ELECTROMAGNETIC FIELDS IN HIGH-ENERGY HEAVY-ION COLLISIONS

PHSD takes into account the dynamical formation and evolution of the electromagnetic fields (EMF) produced by all chargeed particles—hadrons as well as quarks—during the time evolution of high-energy nucleus-nucleus and proton-nucleus collisions [32,65]. To obtain a consistent solution of quasiparticle and electromagnetic field evolution, the off-shell transport equation and the Maxwell equations for the electric field $\boldsymbol{E}$ and the magnetic field $\boldsymbol{B}$ are solved consistently. The electric and magnetic fields can be expressed in terms of the electromagnetic four-vector potential $A_\mu = (\Phi, \mathbf{A})$:

$$\boldsymbol{E} = -\nabla\Phi - \frac{\partial \boldsymbol{A}}{\partial t}, \quad \boldsymbol{B} = \nabla \times \boldsymbol{A}. \tag{1}$$

From the Maxwell equations, we obtain the wave equation for the potentials, whose solution for arbitrarily pointlike moving charges is given by the Liénard-Wiechert potentials. Inserting them into Eq. (1), the retarded electric and magnetic fields at position $\boldsymbol{r}$, generated by a pointlike source charge e at position $\boldsymbol{r}'(t)$ with velocity $\boldsymbol{v}(t)$, are given by

$$\boldsymbol{E}(\boldsymbol{r},t) = \frac{e}{4\pi}\left\{\frac{\boldsymbol{n}-\boldsymbol{\beta}}{\kappa^3\gamma^2R^2} + \frac{\boldsymbol{n}\times[(\boldsymbol{n}-\boldsymbol{\beta})\times\dot{\boldsymbol{\beta}}]}{\kappa^3 cR}\right\}_{\text{ret}}, \tag{2}$$

$$\boldsymbol{B}(\boldsymbol{r},t) = \{\boldsymbol{n}\times\boldsymbol{E}(\boldsymbol{r},t)\}_{\text{ret}}, \tag{3}$$

where $\boldsymbol{R} = \boldsymbol{r} - \boldsymbol{r}'$ with $\boldsymbol{r}' \equiv \boldsymbol{r}(t')$ being the relative position, $\boldsymbol{n} = \boldsymbol{R}/R$ is the unit vector. $\boldsymbol{\beta} = \boldsymbol{v}/c$ and $\dot{\boldsymbol{\beta}} = \mathrm{d}\boldsymbol{\beta}/\mathrm{d}t$ are related to the velocity and acceleration of the particle respectively, and $\kappa = 1 - \boldsymbol{n}\cdot\boldsymbol{\beta}$. All the quantities inside the braces with subscript "ret" have to be evaluated at times t' that are solutions of the retardation equation $t' - t + \boldsymbol{R}(t')/c = 0$. From Eq. (2), we can find that retarded electromagnetic fields from moving charges are divided into two contributions. The first term represents "velocity fields," which are Coulomb fields. The second term describes "acceleration fields," which are interpreted as radiation fields decaying for large distances as R^{-1} [75].

Solving the full equation in the time-dependent case is very complicated. If we neglect the second term "acceleration fields" from Eq. (2), then the remaining term will be the field produced by a charge in uniform motion. Then, considering that in a nuclear collision the total electric and magnetic field is a superposition of the fields produced from all moving charges, one can obtain the final equations implemented in the PHSD transport equation:

$$e\boldsymbol{E}(\boldsymbol{r},t) = \sum_i \frac{\mathrm{sgn}(q_i)\alpha_{em}\boldsymbol{R}_i(t)\left(1-\beta_i^2\right)}{\left\{[\boldsymbol{R}_i(t)\cdot\boldsymbol{\beta}_i]^2 + R_i(t)^2\left(1-\beta_i^2\right)\right\}^{3/2}}, \tag{4}$$

$$e\boldsymbol{B}(\boldsymbol{r},t) = \sum_i \frac{\mathrm{sgn}(q_i)\alpha_{em}\boldsymbol{\beta}_i\times\boldsymbol{R}_i(t)\left(1-\beta_i^2\right)}{\left\{[\boldsymbol{R}_i(t)\cdot\boldsymbol{\beta}_i]^2 + R_i(t)^2\left(1-\beta_i^2\right)\right\}^{3/2}}, \tag{5}$$

where $\alpha_{em} = e^2/4\pi \simeq 1/137$ is the electromagnetic fine-structure constant, and the summation of i runs over all charge particles with charge q_i. The quasiparticle propagation in the electromagnetic field is calculated by the Lorentz force:

$$\left(\frac{\mathrm{d}\boldsymbol{p}_i}{\mathrm{d}t}\right)_{em} = q_i(\boldsymbol{E} + \boldsymbol{\beta}_i\times\boldsymbol{B}). \tag{6}$$

For details of the electromagnetic field production and propagation in high-energy heavy ion collisions within PHSD, we refer the reader to [32,36,61–65]. It is important to mention that the time evolution of the electromagnetic fields computed within PHSD accounts naturally for the electric conductivity σ_{el} of the system. On the other hand, σ_{el} can be computed in PHSD as the response of a strongly interacting system in equilibrium with an external electric field [76]. We note that σ_{el} in PHSD (due to the DQPM) is temperature dependent [77,78], i.e., the ratio σ_{el}/T rises with T in line with lattice QCD data [79,80]. The scattering cross section of heavy quarks with thermal partons might be modified in the presence of electromagnetic fields. The effects of EM field modified interactions or scatterings of heavy quarks are not included in the present study.

IV. RESULTS

Within the PHSD transport approach we proceed to evaluate the heavy quark directed flow,

$$v_1 = \langle\cos(\phi)\rangle = \left\langle\frac{p_x}{p_T}\right\rangle, \tag{7}$$

considered to be a novel observable to probe the EMF produced in high-energy nucleus-nucleus collisions, where ϕ is

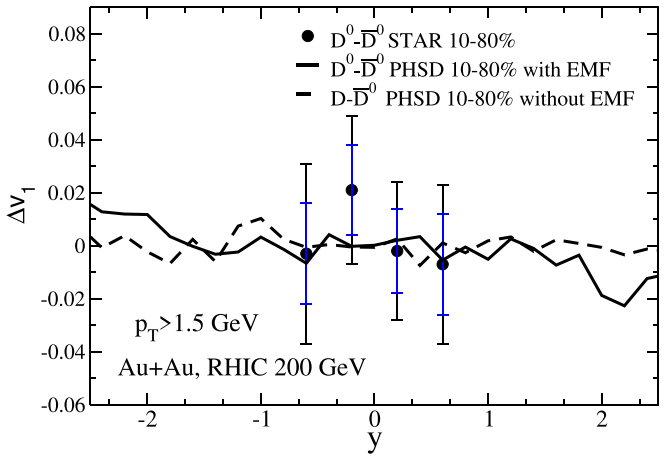

FIG. 1. Variation of the directed flow splitting Δv_1 as a function of rapidity for 10–80% central Au + Au collisions at the highest RHIC energy, $\sqrt{s_{NN}} = 200$ GeV. The experimental data of the STAR Collaboration are taken from Ref. [42].

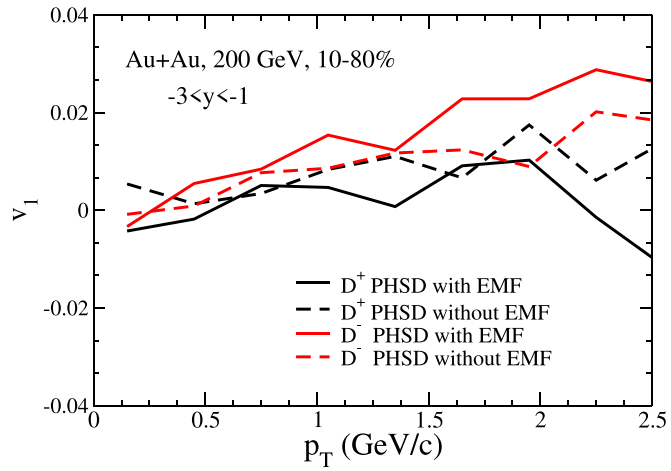

FIG. 2. Directed flow v_1 of D^+ and D^- mesons as a function of p_T for 0–80% central Au + Au collisions at $\sqrt{s_{NN}} = 200$ GeV for $-3 < y < -1$.

the azimuthal angle with respect to the reaction plane. We will also compute the D meson elliptic flow,

$$v_2 = \langle \cos(2\phi) \rangle = \left\langle \frac{p_x^2 - p_y^2}{p_x^2 + p_y^2} \right\rangle, \tag{8}$$

a measure of the anisotropy in the angular distribution of the D meson, to study the influence of the EMF on the elliptic flow.

In Fig. 1 we show the variation of the directed flow splitting, $\Delta v_1 = v_1(D^0) - v_1(\overline{D^0})$, as a function of rapidity for the highest RHIC energy in comparison with the STAR data [42]. We computed the splitting to exclude the contribution to the directed flow from the bulk evolution and to highlight only the effect coming from the EMF. D^0 and $\overline{D^0}$, being neutral, are produced by hadronization of c and $\bar{c}$ quarks respectively. Hence, Δv_1 of the D^0 and $\overline{D^0}$ mesons, if any, is driven by the c and $\bar{c}$ quarks. We find a very mild effect of the EMF on the D meson directed flow, mainly at larger rapidity, which is consistent with the available STAR data. Within the current accuracy, it is almost zero in the rapidity range explored in the STAR measurement. However, at large backward rapidity, $\Delta v_1(y)$ gets a positive contribution from the electromagnetic fields and a negative contribution at larger forward rapidity. We obtain a negative slope of Δv_1 at the highest RHIC energy.

In Ref. [35], the magnitude of the computed v_1 splitting ranges from approximately 0.005 to 0.013 at rapidity -1.8 for different values of the electrical conductivity. For an electrical conductivity of 0.023 fm^{-1}, the splitting is about 0.01. Within the PHSD framework, the magnitude of the splitting at rapidity 2 is around 0.01. However, in PHSD, the electrical conductivity is temperature dependent and is consistent with lattice QCD results. In Ref. [40], the magnitude of the splitting is about 0.005 at rapidity -1 for an electrical conductivity of 0.023 fm^{-1}. In Ref. [34], the magnitude of the splitting is approximately 0.011 at rapidity 1.6 for an electrical conductivity of 0.023 fm^{-1}. However, this calculation was performed for 0–80% centrality using constant drag coefficient.

The directed flow of heavy quarks is an order of magnitude larger than that of light quarks because heavy quarks act as nonequilibrium probes, retaining memory of their interaction history. If heavy quarks are artificially driven toward thermalization by increasing their interaction strength (i.e., enhancing the drag and diffusion coefficients), their directed flow decreases and approaches that of light quarks [33]. High-p_T charm quarks undergo fewer collisions compared to low-p_T charm quarks. High-p_T heavy quarks remain far from thermal equilibrium compared to low-p_T ones, making them more sensitive to electromagnetic fields.

In Fig. 2 we show the directed flow, v_1, of D^+ and D^- as a function p_T in backward rapidity ($-3 \leqslant y \leqslant -1$) with and without EMF. D^+ and D^- mesons are produced by hadronization of c and $\bar{c}$ quarks respectively, like the D^0 and $\overline{D^0}$ mesons. We observe a splitting in the v_1 of D^+ and D^- mesons due to the presence of the EMF in the given rapidity window. We find that the v_1 splitting as a function of p_T is nonzero and is quite substantial, in contrast to the v_1 splitting as a function of rapidity. The splitting of the D meson directed flow as a function of p_T, if measured in future experiments, can act as a novel probe of the produced EMF.

We also computed the D meson elliptic flow v_2 in the PHSD transport approach with and without EMF to highlight the possible effect of the EMF on D meson elliptic flow. In Fig. 3 we present the elliptic flow of D^0 and $\overline{D^0}$ as a function of p_T with and without EMF. We observe that the impact of the EMF on the D meson elliptic flow is negligible.

In Fig. 4 we present the variation of the elliptic flow of D^+ and D^- as a function of p_T with and without EMF. We find that the impact of the EMF of the D meson elliptic flow is small.

V. SUMMARY AND OUTLOOK

We have studied the dynamics of charm quarks in QCD matter produced in nucleus-nucleus collisions at the highest RHIC energy, taking into account the impact of

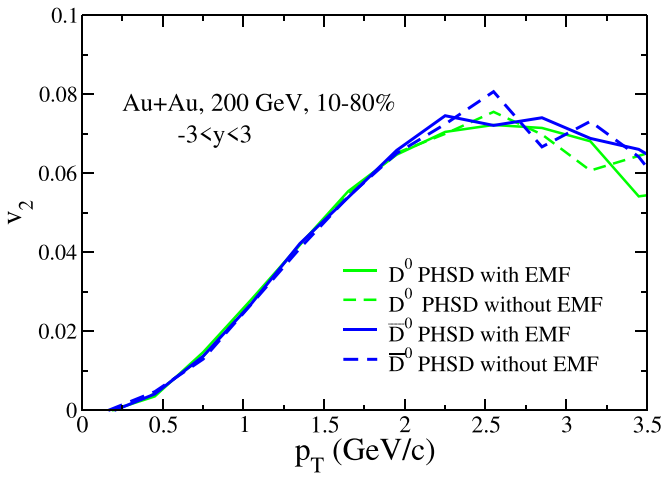

FIG. 3. Elliptic flow v_2 of D^0 and $\overline{D}^0$ mesons as a function p_T for 10–80% central Au + Au collisions at the highest RHIC energy $\sqrt{s_{NN}} = 200$ GeV.

electromagnetic fields within the PHSD transport approach, a microscopic covariant dynamical approach for strongly interacting matter formulated on the basis of off-shell Kadanoff-Baym equations. PHSD can describe heavy quark observables, the nuclear suppression factor (R_{AA}), and elliptic flow (v_2), at both RHIC and LHC energies. In the present study, the initial EMF created high energy heavy-ion collisions due to both the spectators and participants is taken into account dynamically within PHSD; the off-shell transport equation and the Maxwell equations for the EMF are solved to obtain a consistent solution of quasiparticle and electromagnetic field evolution. The electromagnetic fields are calculated according to the retarded Lienard-Wiechert equations for a charge moving with a certain velocity, then summed over all the charged quasiparticles in the medium, both participants and spectators. The time evolution of the EMF computed within PHSD naturally accounts for the electric conductivity $\sigma_{\rm el}$ of the system, which is temperature dependent and in line with the lattice results.

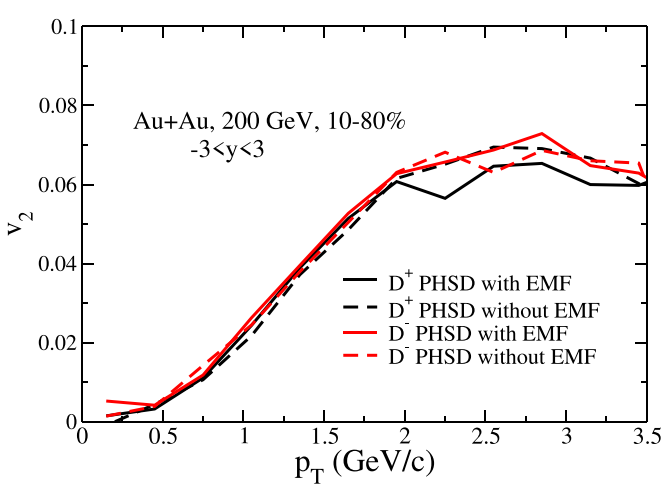

FIG. 4. Elliptic flow v_2 of D^+ (upper) and D^- mesons (lower) as a function p_T for 10–80% central Au + Au collisions at $\sqrt{s_{NN}}$ 200 GeV.

The measured slope of the D meson directed flow splitting a both RHIC and LHC is a subject of high contemporary interest. None of the existing model calculations can describe the slope simultaneously for both RHIC and LHC energies. In this present calculation, we have made an attempt to study heavy quark dynamics in the background EMF at RHIC energy in a self-consistent way, hence relaxing some of the approximations made in earlier studies by considering only spectators to evaluate the EMF and including a constant electric conductivity $\sigma_{\rm el}$.

We have computed the splitting of the directed flow, $\Delta v_1 = v_1(D^0) - v_1(\overline{D^0})$, within the PHSD transport approach and compared the results with the available STAR data at the highest RHIC energy. PHSD can describe the STAR data; however, the impact of the EMF is quite mild, and it is almost zero in the rapidity ranges explored in the STAR measurement. However, the impact of the EMF for large forward-backward rapidity is quite visible. We obtain a negative slope of Δv_1 at the highest RHIC energy, though the magnitude of the splitting obtained within PHSD is small in comparison with other models. We have also evaluated the D meson directed flow as a function of p_T.

We have observed that the D meson directed flow splitting as a function of transverse momentum at a certain rapidity range is very sensitive to the EMF. If measured in an experiment, it can act as a novel probe to characterize the produced EMF at high-energy heavy-ion collisions. We have also computed the possible impact of EMF on D meson elliptic flow.

We have found that the impact of the EMF on the D meson elliptic flow is negligible. This indicates that the heavy quark directed flow is the only observable to characterize the EMF. However, the directed flow as a function of p_T is more sensitive to the electromagnetic field. It will be interesting to perform a similar study in the presence of an electromagnetic field at LHC energy. We will address this in a forthcoming article.

ACKNOWLEDGMENTS

S.K.D. acknowledges support from SERB IRE fellowship, India, under Project No. SIR/2022/000231. The authors thank to Lucia Oliva for inspiring discussions. We also acknowledge support by the Deutsche Forschungsgemeinschaft (DFG) through the Grant No. CRC-TR211 “Strong-interaction matter under extreme conditions” (Project No. 315477589–TRR 211).

DATA AVAILABILITY

The data that support the findings of this article are not publicly available upon publication because it is not technically feasible and/or the cost of preparing, depositing, and hosting the data would be prohibitive within the terms of this research project. The data are available from the authors upon reasonable request.

[1] E. V. Shuryak, Nucl. Phys. A **750**, 64 (2005).
[2] B. V. Jacak and B. Muller, Science **337**, 310 (2012).
[3] F. Prino and R. Rapp, J. Phys. G **43**, 093002 (2016).
[4] A. Andronic *et al.*, Eur. Phys. J. C **76**, 107 (2016).
[5] A. Beraudo *et al.*, Nucl. Phys. A **979**, 21 (2018).
[6] G. Aarts *et al.*, Eur. Phys. J. A **53**, 93 (2017).
[7] S. Cao *et al.*, Phys. Rev. C **99**, 054907 (2019).
[8] X. Dong and V. Greco, Prog. Part. Nucl. Phys. **104**, 97 (2019).
[9] Y. Xu *et al.*, Phys. Rev. C **99**, 014902 (2019).
[10] S. K. Das, J. M. Torres-Rincon, and R. Rapp, Phys. Rep. **1129-1131**, 1 (2025).
[11] H. van Hees, V. Greco, and R. Rapp, Phys. Rev. C **73**, 034913 (2006).
[12] H. van Hees, M. Mannarelli, V. Greco, and R. Rapp, Phys. Rev. Lett. **100**, 192301 (2008).
[13] P. B. Gossiaux and J. Aichelin, Phys. Rev. C **78**, 014904 (2008).
[14] P. B. Gossiaux, R. Bierkandt, and J. Aichelin, Phys. Rev. C **79**, 044906 (2009).
[15] S. K. Das, J.-e. Alam, and P. Mohanty, Phys. Rev. C **82**, 014908 (2010).
[16] W. M. Alberico, A. Beraudo, A. De Pace, A. Molinari, M. Monteno, M. Nardi, and F. Prino, Eur. Phys. J. C **71**, 1666 (2011).
[17] T. Lang, H. van Hees, J. Steinheimer, G. Inghirami, and M. Bleicher, Phys. Rev. C **93**, 014901 (2016).
[18] J. Uphoff, O. Fochler, Z. Xu, and C. Greiner, Phys. Rev. C **84**, 024908 (2011).
[19] M. He, R. J. Fries, and R. Rapp, Phys. Rev. Lett. **110**, 112301 (2013).
[20] J. Uphoff, O. Fochler, Z. Xu, and C. Greiner, Phys. Lett. B **717**, 430 (2012).
[21] S. K. Das, F. Scardina, S. Plumari, and V. Greco, Phys. Rev. C **90**, 044901 (2014).
[22] S. K. Das, F. Scardina, S. Plumari, and V. Greco, Phys. Lett. B **747**, 260 (2015).
[23] T. Song, H. Berrehrah, D. Cabrera, J. M. Torres-Rincon, L. Tolos, W. Cassing, and E. Bratkovskaya, Phys. Rev. C **92**, 014910 (2015).
[24] M. Nahrgang, J. Aichelin, S. Bass, P. B. Gossiaux, and K. Werner, Phys. Rev. C **91**, 014904 (2015).
[25] T. Song, H. Berrehrah, D. Cabrera, W. Cassing, and E. Bratkovskaya, Phys. Rev. C **93**, 034906 (2016).
[26] S. Cao, T. Luo, G.-Y. Qin, and X.-N. Wang, Phys. Rev. C **94**, 014909 (2016).
[27] F. Scardina, S. K. Das, V. Minissale, S. Plumari, and V. Greco, Phys. Rev. C **96**, 044905 (2017).
[28] Y. Xu, J. E. Bernhard, S. A. Bass, M. Nahrgang, and S. Cao, Phys. Rev. C **97**, 014907 (2018).
[29] S. Plumari, V. Minissale, S. K. Das, G. Coci, and V. Greco, Eur. Phys. J. C **78**, 348 (2018).
[30] R. Katz, C. A. G. Prado, J. Noronha-Hostler, J. Noronha, and A. A. P. Suaide, Phys. Rev. C **102**, 024906 (2020).
[31] V. Skokov, A. Y. Illarionov, and V. Toneev, Int. J. Mod. Phys. A **24**, 5925 (2009).
[32] V. Voronyuk, V. D. Toneev, W. Cassing, E. L. Bratkovskaya, V. P. Konchakovski, and S. A. Voloshin, Phys. Rev. C **83**, 054911 (2011).
[33] S. K. Das, S. Plumari, S. Chatterjee, J. Alam, F. Scardina, and V. Greco, Phys. Lett. B **768**, 260 (2017).
[34] S. Chatterjee and P. Bozek, Phys. Lett. B **798**, 134955 (2019).
[35] L. Oliva, S. Plumari, and V. Greco, J. High Energy Phys. 05 (2021) 034.
[36] L. Oliva, Eur. Phys. J. A **56**, 255 (2020).
[37] A. Dubla, U. Gürsoy, and R. Snellings, Mod. Phys. Lett. A **35**, 2050324 (2020).
[38] Y. Sun, S. Plumari, and V. Greco, Phys. Lett. B **816**, 136271 (2021).
[39] A. Beraudo, A. De Pace, M. Monteno, M. Nardi, and F. Prino, J. High Energy Phys. 05 (2021) 279.
[40] Z.-F. Jiang, S. Cao, W.-J. Xing, X.-Y. Wu, C. B. Yang, and B.-W. Zhang, Phys. Rev. C **105**, 054907 (2022).
[41] Y. Sun, S. Plumari, and S. K. Das, Phys. Lett. B **843**, 138043 (2023).
[42] J. Adam *et al.* (STAR Collaboration), Phys. Rev. Lett. **123**, 162301 (2019).
[43] S. Acharya *et al.* (ALICE Collaboration), Phys. Rev. Lett. **125**, 022301 (2020).
[44] K. Fukushima, K. Hattori, H.-U. Yee, and Y. Yin, Phys. Rev. D **93**, 074028 (2016).
[45] M. Kurian, S. K. Das, and V. Chandra, Phys. Rev. D **100**, 074003 (2019).
[46] M. Kurian, V. Chandra, and S. K. Das, Phys. Rev. D **101**, 094024 (2020).
[47] A. Bandyopadhyay, J. Liao, and H. Xing, Phys. Rev. D **105**, 114049 (2022).
[48] D. Dey and B. k. Patra, Phys. Rev. D **109**, 116008 (2024).
[49] A. Bandyopadhyay, Phys. Rev. D **109**, 034013 (2024).
[50] S. Satapathy, S. De, J. Dey, and S. Ghosh, Phys. Rev. C **109**, 024904 (2024).
[51] D. Dey, A. Bandyopadhyay, S. K. Das, S. Dash, V. Chandra, and B. K. Nandi, Phys. Rev. D **112**, 016011 (2025).
[52] W. Cassing and E. L. Bratkovskaya, Phys. Rev. C **78**, 034919 (2008).
[53] W. Cassing, Eur. Phys. J. Spec. Top. **168**, 3 (2009).
[54] W. Cassing and E. L. Bratkovskaya, Nucl. Phys. A **831**, 215 (2009).
[55] E. L. Bratkovskaya, W. Cassing, V. P. Konchakovski, and O. Linnyk, Nucl. Phys. A **856**, 162 (2011).
[56] O. Linnyk, E. L. Bratkovskaya, and W. Cassing, Prog. Part. Nucl. Phys. **87**, 50 (2016).
[57] P. Moreau, O. Soloveva, L. Oliva, T. Song, W. Cassing, and E. Bratkovskaya, Phys. Rev. C **100**, 014911 (2019).
[58] W. Cassing, Nucl. Phys. A **795**, 70 (2007).
[59] W. Cassing, Nucl. Phys. A **791**, 365 (2007).
[60] O. Soloveva, D. Fuseau, J. Aichelin, and E. Bratkovskaya, Phys. Rev. C **103**, 054901 (2021).
[61] V. D. Toneev, V. Voronyuk, E. L. Bratkovskaya, W. Cassing, V. P. Konchakovski, and S. A. Voloshin, Phys. Rev. C **85**, 034910 (2012).
[62] V. D. Toneev, V. P. Konchakovski, V. Voronyuk, E. L. Bratkovskaya, and W. Cassing, Phys. Rev. C **86**, 064907 (2012).
[63] V. Voronyuk, V. D. Toneev, S. A. Voloshin, and W. Cassing, Phys. Rev. C **90**, 064903 (2014).
[64] V. D. Toneev, V. Voronyuk, E. E. Kolomeitsev, and W. Cassing, Phys. Rev. C **95**, 034911 (2017).
[65] L. Oliva, P. Moreau, V. Voronyuk, and E. Bratkovskaya, Phys. Rev. C **101**, 014917 (2020).
[66] M. Cacciari, S. Frixione, N. Houdeau, M. L. Mangano, P. Nason, and G. Ridolfi, J. High Energy Phys. 10 (2012) 137.
[67] K. J. Eskola, H. Paukkunen, and C. A. Salgado, J. High Energy Phys. 04 (2009) 065.

[68] H. Berrehrah, E. Bratkovskaya, W. Cassing, P. B. Gossiaux, J. Aichelin, and M. Bleicher, Phys. Rev. C **89**, 054901 (2014).
[69] C. Peterson, D. Schlatter, I. Schmitt, and P. M. Zerwas, Phys. Rev. D **27**, 105 (1983).
[70] L. M. Abreu, D. Cabrera, F. J. Llanes-Estrada, and J. M. Torres-Rincon, Ann. Phys. **326**, 2737 (2011).
[71] T. Song, H. Berrehrah, J. M. Torres-Rincon, L. Tolos, D. Cabrera, W. Cassing, and E. Bratkovskaya, Phys. Rev. C **96**, 014905 (2017).
[72] T. Song, W. Cassing, P. Moreau, and E. Bratkovskaya, Phys. Rev. C **97**, 064907 (2018).
[73] T. Song, P. Moreau, Y. Xu, V. Ozvenchuk, E. Bratkovskaya, J. Aichelin, S. A. Bass, P. B. Gossiaux, and M. Nahrgang, Phys. Rev. C **101**, 044903 (2020).
[74] T. Song, I. Grishmanovskii, O. Soloveva, and E. Bratkovskaya, Phys. Rev. C **110**, 034906 (2024).
[75] L. D. Landau and E. M. Lifschits, *The Classical Theory of Fields*, Course of Theoretical Physics (Pergamon, Oxford, 1975), Vol. 2.
[76] W. Cassing, O. Linnyk, T. Steinert, and V. Ozvenchuk, Phys. Rev. Lett. **110**, 182301 (2013).
[77] O. Soloveva, P. Moreau, and E. Bratkovskaya, Phys. Rev. C **101**, 045203 (2020).
[78] J. A. Fotakis, O. Soloveva, C. Greiner, O. Kaczmarek, and E. Bratkovskaya, Phys. Rev. D **104**, 034014 (2021).
[79] B. B. Brandt, A. Francis, H. B. Meyer, and H. Wittig, J. High Energy Phys. 03 (2013) 100.
[80] G. Aarts, C. Allton, A. Amato, P. Giudice, S. Hands, and J.-I. Skullerud, J. High Energy Phys. 02 (2015) 186.